HHS Public Access

Author manuscript

Genes Chromosomes Cancer. Author manuscript; available in PMC 2018 June 01.

Published in final edited form as:

Genes Chromosomes Cancer. 2017 June ; 56(6): 501–510. doi:10.1002/gcc.22454.

ETV transcriptional upregulation is more reliable than RNA sequencing algorithms and FISH in diagnosing round cell sarcomas with *CIC* gene rearrangements

Yu-Chien Kao[1,2], **Yun-Shao Sung**[1], **Chun-Liang Chen**[1], **Lei Zhang**[1], **Brendan C Dickson**[3], **David Swanson**[3], **Sumathi Vaiyapuri**[4], **Farida Latif**[5], **Abdullah Alholle**[6], **Shih-Chiang Huang**[7], **Jason L. Hornick**[8], and **Cristina R Antonescu**[1]

[1]Department of Pathology, Memorial Sloan Kettering Cancer Center, New York, New York, USA

[2]Department of Pathology, Shuang Ho Hospital, Taipei Medical University, Taipei, Taiwan

[3]Department of Pathology, Mount Sinai Hospital, Toronto, Canada

[4]Department of Musculoskeletal Pathology, The Royal Orthopaedic Hospital NHS Foundation Trust, Birmingham, United Kingdom

[5]Department of Human Molecular Genetics, School of Clinical and Experimental Medicine, The Medical School University of Birmingham Edgbaston, Birmingham, United Kingdom

[6]Institute of Cancer and Genomic Sciences College of Medical and Dental Sciences University of Birmingham, Birmingham, United Kingdom

[7]Department of Anatomical Pathology, Chang Gung Memorial Hospital, Chang Gung University College of Medicine, Taoyuan, Taiwan

[8]Department of Pathology, Brigham and Women's Hospital and Harvard Medical School, Boston, Massachusetts, USA

Abstract

CIC rearrangements have been reported in two-thirds of *EWSR1*-negative small blue round cell tumors (SBRCTs). However, a number of SBRCTs remain unclassified despite exhaustive analysis. Fourteen SBRCTs lacking driver genetic events by RNA sequencing (RNAseq) analysis were collected. Unsupervised hierarchical clustering was performed using samples from our RNAseq database, including 13 SBRCTs with non-*CIC* genetic abnormalities and 2 *CIC*-rearranged angiosarcomas among others. Remarkably, all 14 study cases showed high mRNA levels of *ETV1/4/5*, and by unsupervised clustering most grouped into a distinct cluster, separate from other tumors. Based on these results indicating a close relationship with *CIC*-rearranged tumors, we manually inspected *CIC* reads in RNAseq data. FISH for *CIC* and *DUX4*

Correspondence: Cristina R Antonescu, MD, Memorial Sloan-Kettering Cancer Center, Pathology Department, 1275 York Ave, New York, NY, USA. antonesc@mskcc.org.

CONFLICT OF INTEREST

The authors declare that they have no conflicts of interest with the contents of this article.

SUPPORTING INFORMATION

Additional Supporting Information may be found in the online version of this article.

abnormalities and immunohistochemical stains for ETV4 were also performed. In the control group, only 2 *CIC*-rearranged angiosarcomas had high *ETV1/4/5* expression. Upon manual inspection of *CIC* traces, 7 of 14 cases showed *CIC-DUX4* fusion reads, 2 cases had *DUX4-CIC* reads, while the remaining 5 were negative. FISH showed *CIC* break-apart in 7 cases, including 5 cases lacking *CIC-DUX4* or *DUX4-CIC* fusion reads on RNAseq manual inspection. However, no *CIC* abnormalities were detected by FISH in 6 cases with *CIC-DUX4* or *DUX4-CIC* reads. ETV4 immunoreactivity was positive in 7 of 11 cases. Our results highlight the underperformance of FISH and RNAseq methods in diagnosing SBRCTs with *CIC* gene abnormalities. The downstream *ETV1/4/5* transcriptional up-regulation appears highly sensitive and specific and can be used as a reliable molecular signature and diagnostic method for *CIC* fusion positive SBRCTs.

1 | INTRODUCTION

CIC-DUX4 gene fusion, resulting from either t(4;19) or t(10;19) translocation, is the most common genetic abnormality detected in *EWSR1*-negative small blue round cell tumors (SBRCTs).[1,2] *CIC-DUX4* sarcomas occur most commonly in young adults within the somatic soft tissues.[1,3–6] Patients with *CIC*-rearranged sarcomas follow a clinically aggressive course, with high metastatic rate and an inferior overall survival compared with the Ewing sarcoma patients.[6,7] Microscopically, *CIC*-fusion positive SBRCTs show more cytologic variability compared with classic Ewing sarcomas, with round to ovoid and occasionally spindle cell histology, showing mild nuclear pleomorphism, prominent nucleoli, and myxoid stroma.[3,5,6] Immunohistochemical reactivity of ETV4 has recently been reported as a useful ancillary tool in supporting the diagnosis, based on the prior evidence that *CIC-DUX4* sarcomas overexpress the PEA3 subfamily of transcription factors, including *ETV1*, *ETV4*, and *ETV5*, both at mRNA and protein levels.[2,4,5,8] RNA in situ hybridization of ETV1/4/5 was also utilized by others.[9] Another adjunct marker in diagnosing *CIC-DUX4* sarcomas is the presence of nuclear immunoreactivity for WT1, which has similar sensitivity but inferior specificity compared with ETV4, being also positive in other round cell tumors, including desmoplastic small round cell tumor, alveolar rhabdomyosarcoma, Wilms tumor, lymphoblastic lymphoma, etc.[4,5]

RNA sequencing (RNAseq) has emerged as a powerful tool in identifying genetic abnormalities and has become the preferred method for novel gene fusion discovery. However, in our experience, a subset of SBRCTs remained unclassified after transcriptome sequencing and detailed bioinformatic algorithm analysis suggesting lack of driving genetic fusion events. Remarkably though, despite the lack of recurrent fusion candidates, this group of SBRCTs had a similar transcriptional signature, including *ETV1/4/5* gene up-regulation, typically seen in the *CIC-DUX4* fusion positive SBRCTs. Based on these findings we employed various molecular methods, such as manual inspection of certain genes of interest, FISH and immunohistochemistry, in order to elucidate their genomic classification and pathogenetic relationship to the more common and well defined *CIC-DUX4* fusion positive group of SBRCT.

2 | MATERIALS AND METHODS

2.1 | Case selection

We collected 14 SBRCTs that were subjected to whole transcriptome sequencing (n = 10) and/or targeted RNA sequencing (n = 5, including one case tested for both platforms), but no driver genetic events were identified. Since *CIC-DUX4* fusions are the most common genetic events among the *EWSR1*-negative SBRCTs, we further examined the RNA sequencing data for *ETV1/4/5* and *WT1* gene expressions, manual inspection of *CIC* sequences, FISH for *CIC* and *DUX4* genetic abnormalities and immunohistochemistry for ETV4.

The patients' cohort had an equal gender distribution and a wide age range at diagnosis (11–66 years old, mean 32.8), with a bimodal distribution in the second to third and 6th to 7th decade of age. The tumors arose predominantly in soft tissues (n = 12): 5 in the trunk, 4 in the extremities, and 3 in the head and neck, with only one case each in the phalangeal bone and brain (Table 1). Within the soft tissue, all except one tumor were deep-seated. One lesion was centered in the subcutaneous tissue (case #13), while another (case #9) involved dermis, subcutaneous tissue, and underlying skeletal muscle. The only bone lesion (case #5) showed a destructive growth in the phalangeal bone, extending to the interphalangeal joint and surrounding soft tissues. The study was approved by the Institutional Review Board.

2.2 | Whole transcriptome sequencing

Total RNA was extracted in cases #1–5 and #8–12 from frozen tissues using RNeasy Plus Mini (Qiagen), followed by mRNA isolation with oligo(dT) magnetic beads and fragmentation by incubation at 94°C in fragmentation buffer (Illumina) for 2.5 minutes. After gel size-selection (350–400 bp) and adapter ligation, the library was enriched by PCR for 15 cycles and purified. Paired-end RNA sequencing at read lengths of 50 or 51 bp was performed with the HiSeq 2000 (Illumina).

2.3 | Targeted RNA sequencing

For cases #6,7,10,13,14 RNA was extracted from formalin-fixed paraffin-embedded (FFPE) tissues using Amsbio's ExpressArt FFPE Clear RNA Ready kit (Amsbio LLC, Cambridge, MA). Fragment length was assessed with an RNA 6000 chip on an Agilent Bioanalyzer (Agilent Technologies, Santa Clara, CA). RNA-seq libraries were prepared using 20–100 ng total RNA with the Trusight RNA Fusion Panel (Illumina, San Diego, CA). Each sample was subjected to targeted RNA sequencing on an Illumina MiSeq at 8 samples per flow cell (~3 million reads per sample).

2.4 | RNA sequencing data analysis

After being independently aligned by STAR (ver 2.3) and BowTie2 against the human reference genome (hg19), the reads were analyzed by FusionSeq, STAR-Fusion, and TopHat-Fusion algorithms for whole transcriptome sequencing data and by Manta-Fusion, STAR-Fusion, and TopHat-Fusion for targeted RNA sequencing data for fusion discovery. No convincing fusion candidates were identified in these samples. The *CIC* gene reads were manually inspected on Integrative Genomics Viewer. Reads with partially mismatched

sequences were examined by BLAT (http://genome.ucsc.edu/cgi-bin/hgBlat? command = start). Similar attempts to investigate *DUX4* were unsuccessful due to lack of reads mapped to *DUX4* region. Expression levels of *CIC, ETV1, ETV4, ETV5*, and *WT1* were evaluated on both RNAseq platforms in comparison to other soft tissue tumors in each platform. The mRNA expression of known *PEA3* family downstream target genes, including *SPRY2, SPRY4, SPRED2, GPR20, DUSP6 GBX2, FGF8, POU5F1, MMP1/2/3/7/9, TWIST1, SNAI1/2, PTGS2, BAX, CCND2, ZEB1, PTK2, PLAU, ICAM1, VEGFA, NOTCH1, NOTCH4*, and *SPP1*[10–19] was investigated from the whole transcriptome sequencing platform, while *FRG1, PITX1, ZSCAN4, RFPL2, TRIM43*, and *LEUTX*, were evaluated as *DUX4* targets.[20–23]

Cases studied by the whole transcriptome sequencing (n = 10) were also subjected to unsupervised hierarchical clustering, together with > 140 samples from our database, mostly sarcomas, including 2 *CIC*-rearranged angiosarcomas[24] and 13 SBRCTs with non-*CIC* genetic abnormalities (6 with *BCOR* internal tandem duplication (ITD), 1 with *YWHAE-NUTM2E*, 1 with *BCOR-CCNB3*, 1 with *EWSR1-ERG*, and 4 Ewing sarcoma cell lines) among others.

A gene expression signature was obtained from the 8 study group SBRCT cases (2 outliers on unsupervised hierarchical clustering excluded) compared with other sarcoma samples available on our whole transcriptome sequencing platform (from Figure 1). It was then compared with the published gene expressions of *CIC-DUX4* SBRCTs (175 gene list, Affymetrix U133A chip) and Ewing sarcomas (95 gene list, Affymetrix Human Gene 1.0 ST arrays).[2] A differentially expressed gene list of 152 genes was obtained from our study group using log2-fold change thresholds of positive 2 or negative 5 and a 0.01 false discovery rate and after eliminating genes that were not represented on all 3 platforms. These 3 expression profiles were then analyzed by Venn diagram and supervised clustering.

2.5 | Fluorescence in situ hybridization (FISH)

FISH for *CIC* break-apart was performed on 4 μm-thick FFPE tissue sections of all cases. *CIC-DUX4* fusion assays were also tested on selected cases. Custom probes were made by bacterial artificial chromosomes (BAC) clones flanking the target genes, according to UCSC genome browser (http://genome.ucsc.edu) and obtained from BACPAC sources of Children's Hospital of Oakland Research Institute (Oakland, CA; http://bacpac.chori.org). Being located at the telomeric end of 4q and 10q chromosomes, no BAC clone was available for design on the telomeric side (3′) of *DUX4* gene. Therefore, for the fusion assay, the reciprocal fusion was used with centromeric *DUX4* (5′) and telomeric *CIC* (3′) BAC clones (Supporting Information Table 1). DNA from each BAC was isolated according to the manufacturer's instructions. The BAC clones were labeled with fluorochromes by nick translation and validated on normal metaphase chromosomes. The slides were deparaffinized, pretreated, and hybridized with denatured probes. After overnight incubation, the slides were washed, stained with DAPI, mounted with an antifade solution, and then examined on a Zeiss fluorescence microscope (Zeiss Axioplan, Oberkochen, Germany) controlled by Isis 5 software (Metasystems).

2.6 | Immunohistochemistry for ETV4

Eleven of 14 cases in the study cohort with available materials were subjected for ETV4 immunostaining. Immunohistochemistry was performed on 4 μm-thick FFPE tissue sections using monoclonal mouse anti-PEA3 (ETV4) antibody (clone 16/sc-113; Santa Cruz, CA, USA; 1:50 dilution) as previously described.[4] The results were interpreted as positive when moderate or strong nuclear stain was present in at least 50% of tumor cells.

2.7 | Reverse transcription-polymerase chain reaction (RT-PCR)

RT-PCR was performed in cases #2 and #8 to validate the *CIC-DUX4* and *DUX4-CIC* fusion transcripts identified by manual inspection of RNAseq data. RNA was extracted from frozen tissues using RNeasy Plus Mini (Qiagen) and reverse transcribed by SuperScript IV First-Strand Synthesis System (Invitrogen). PCR was performed by Advantage 2 PCR kit (Clontech, Mountain View, CA) with forward primer on *DUX4* intron 1 (5′-GGAAGAATACCGGGCTCTGCTG-3′) (uc001lns.2) and reverse primer on *CIC* exon 20 (5′-CAAACTGGAGAGGAC-GAAATGG-3′) (ENST00000575354.6) for case #8; forward primer on *CIC* exon 20 (5′-CTGACCCCACCTCACCCAGCTC-3′) and reverse primer on *DUX4* intron 1 (5′-GCAGAGCCCGGTATTCTTCC-3′) for case #2. The reactions were run at 65°C annealing temperature for 35 cycles. The PCR products were analyzed by gel electrophoresis and Sanger sequencing.

3 | RESULTS

3.1 | Significant *ETV1/4/5* mRNA up-regulation is the hallmark of SBRCTs lacking other fusions by RNA sequencing

Remarkably all 14 SBRCTs lacking fusion candidates by whole transcriptome or targeted RNA sequencing showed consistent up-regulation of *ETV1, ETV4*, and *ETV5* mRNA expression levels, compared with other SBRCTs with known non-*CIC* genetic alterations and various soft tissue tumors in each of the platform analyzed (Figure 1A). *WT1* mRNA was also up-regulated in the majority of cases (Figure 1A). In case #10, both whole transcriptome and targeted RNAseq data showed similar up-regulation of *ETV1/4/5* and *WT1* expression. None of the cases showed *CIC* mRNA overexpression, which was at similar low levels with the SBRCT control group (data not shown). Analysis of downstream targets of *PEA3* gene family revealed up-regulated *SPRED2* (target of ETV1), *CCND2* and *NOTCH1* (targets of ETV4)[12,14] expressions (Supporting Information Figure 1). None of the potential *DUX4* gene targets examined was significantly up-regulated.

Unsupervised hierarchical clustering of a large number of cases available on the whole transcriptome RNAseq platform showed that 8 of 10 SBRCTs sharing a PEA3 upregulated signature formed a tight genomic cluster, supporting a common transcriptional profile in these tumors (Figure 1B). In the control group, 2 *CIC*-rearranged angiosarcomas also had high levels of *ETV1/4/5* expression, clustering together with the study cohort. SBRCTs with non-*CIC* genetic abnormalities had low levels of *ETV1/4/5* and *WT1* mRNA and clustered separately as distinct groups. A group of SDHB-deficient pediatric gastrointestinal stromal tumors (GIST) not initially included among the control group showed up-regulation

restricted to *ETV1*, but not *ETV4/5*, as previously reported,[10] clustering separately from the SBRCTs.

The Venn diagram was used to compare the gene expression overlap between the SBRCT study group (RNAseq), *CIC-DUX4* (Affymetrix U133A) and Ewing sarcoma (Affymetrix Human Gene 1.0 ST arrays). There was a 64-gene overlap between the study group and *CIC-DUX4* tumors signature on Affymetrix U133A platform (Supporting Information Figure 2A), while only 1 gene was in common with the Ewing sarcoma gene list. Supervised clustering using the SBRCT study group 152 gene-list was able to group the 8 samples from the study cohort as well as the known *CIC-DUX4* tumors, but not the Ewing sarcoma samples (Supporting Information Figure 2B).

3.2 | *CIC-DUX4* fusion junction or chimeric reads are identified only through manual inspection of RNAseq in a subset of SBRCT with PEA3 gene signature

Manual inspection of the *CIC* sequences showed *CIC-DUX4* reads in 7 cases: 5 with fusion junction reads (individual reads spanning both *CIC* and *DUX4* sequences and the fusion junctions) and 2 with only chimeric reads (*CIC* and *DUX4* sequences on each of the paired-end reads) (Supporting Information Table 2). Consistently all cases showed *CIC* breakpoints within the coding region of the last exon (exon 20) (Figure 2A), while *DUX4* breakpoints were scattered in exons 1–2 or intron 1 (sequence reference: uc001lns.2). *DUX4* pseudogene has high sequence homology on both chromosomes 4q35 and 10q26. Thus based on the *CIC-DUX4* chimeric/fusion junction reads available, a distinction between *DUX4* sequence on chromosomes 4 or 10 could not be made, with the exception of case #7 which showed a *DUX4* sequence matching to chromosome 10. The projected amino acids of the CIC-DUX4 fusion protein were in-frame in all cases except two (cases #6, 7), in which fusion of *CIC* exon 20 to *DUX4* resulted in a stop codon right after the fusion junction (Figure 2C). RT-PCR confirmed *CIC-DUX4* fusion in case #2 (Figure 2B).

Additionally, 2 cases without *CIC-DUX4* reads by manual inspection had instead the reciprocal *DUX4-CIC* fusion junction reads (cases #8,9, Table 1, Supporting Information Table 2). In case # 8 the *DUX4* sequence matched to chromosome 10, while in case #9 the distinction between chromosomes 4/10 could not be made. The fusion junctions showed *DUX4* intron 1 fused to *CIC* exon 20 (3′ UTR region in case #8, coding region in case #9) (Figure 2A). *DUX4-CIC* fusion transcript was confirmed by RT-PCR in case #8 with available material (Figure 2B).

The remaining 5 cases (cases #10–14) were negative for *CIC-DUX4* or *DUX4-CIC* reads. Among them, case#10 showed *CIC* gene being fused to an un-annotated region in chromosome 17q21.31 (genomic position: chr17:41419677, GRCh37/hg19). The remaining 4 cases showed only wild-type sequence of *CIC*. No association between the fusion reads types (*CIC-DUX4, DUX4-CIC*, or none) and the mRNA expression level of *ETV1/4/5* was noted. No *CIC-DUX4* or *DUX4-CIC* reads were found in the control group of SBRCTs by manual inspection or algorithm analysis.

3.3 | FISH *CIC* gene rearrangements are detected in half of SBRCTs with PEA3 up-regulation

FISH assays detected *CIC* break-apart in 7 of 13 cases (Table 1), including 2 cases with *CIC-DUX4* reads (case #3,6), 1 case with *CIC* fused to a un-annotated region in chromosome 17 (case #10), and 4 cases (case #11–14) lacking *CIC* abnormalities by either manual inspection or algorithm RNAseq analyses. One case failed to show hybridized signals due to tissue decalcification. Fusion FISH assays confirmed telomeric *CIC* and centromeric *DUX4* (4q35) fusions in 2 cases (cases# 11, 12), while no association between *CIC* and *DUX4* (both 4q35 and 10q26 loci) was found in cases #13, 14. As expected, case #10 showing a *CIC* fusion to an un-annotated chromosome 17 region was negative for t(4;19)—*CIC-DUX4* fusion FISH assay, while the t(10;19) fusion was not evaluable due to a centromeric *DUX4* (10q26.3) deletion noted by FISH. The 2 remaining cases with *CIC-DUX4* reads and *CIC* rearrangements by FISH could not be evaluated further by fusion FISH assays due to a telomeric deletion of *CIC* (case #6) or low percentage (10%–20%) of *CIC*-rearranged tumor cells (case #3). The remaining 6 cases negative for *CIC* abnormalities by FISH displayed *CIC-DUX4* or *DUX4-CIC* reads by RNAseq manual inspection.

3.4 | The morphologic spectrum and ETV4 immunoreactivity of SBRCTs with *ETV1/4/5* up-regulation is similar to *CIC-DUX4* fusion positive sarcoma

Histologically, the tumors were mostly composed of small blue round cells with mild variation in nuclear size and shape (Figure 3A). Three cases (case #1, 6, 13) showed a mixture of spindle and round cells (Figure 3B), while 2 cases (case # 5, 9) had plump epithelioid cells with palely eosinophilic cytoplasm (Figure 3C). Necrosis was present in 8 cases, either as spotty areas or confluent geographic necrosis. Small to moderate amount of myxoid stroma was frequently observed (n = 9), either separating tumor cells or admixed with necrotic debris (n = 5), and/or forming microcystic spaces (n = 4) (Figure 3D,E). The tumor cells showed vesicular chromatin and prominent nucleoli in the majority of cases, while an evenly distributed chromatin pattern with inconspicuous nucleoli was seen in areas (n = 2) or as the predominant cytologic feature in one case. Immunohistochemically, ETV4 stain was positive in 7 of 11 cases tested, with moderate to strong intensity and diffuse to patchy staining (Figure 3F). Among the 7 positive cases, 3 had *CIC-DUX4* reads by RNAseq data, while remaining had *CIC* rearrangement by FISH but no confirmatory fusion/chimeric reads. The 4 cases negative for ETV4 immmunostaining had either *CIC-DUX4* reads (n = 2), *DUX4-CIC* reads (n = 1), or *CIC-DUX4* fusion confirmed by FISH (n = 1). The mRNA expression levels of *ETV1*, *ETV4*, and *ETV5* in these 4 cases were markedly up-regulated compared with other tumor types (Figure 1A, asterisks). Further WT1 stains in these 4 cases were unsuccessful, which raised the possibility of tissue failure in these samples. CD99 staining results available in 11 cases showed positivity with variable extent and intensity.

4 | DISCUSSION

In this study, we report a series of 14 undifferentiated round cell sarcomas that remained unclassified by RNAseq fusion discovery algorithms but surprisingly showed a distinct transcriptional *ETV1/4/5* upregulation, similar to the reported mRNA signature of *CIC-*

DUX4 sarcomas. Upon further investigation, most cases showed some evidence of *CIC-DUX4* fusions by manual inspection of RNAseq data or *CIC* rearrangements by FISH. *DUX4* gene is located within the D4Z4 macrosatellite repeat region (11–100 copies of the repeat units) of the chromosomes 4 and 10 subtelomeric regions.[25] As the fusion discovery algorithms involve filtering out artifacts and noises, including repetitive sequences,[26] the false-negative RNAseq results are most likely related to the repetitive nature of *DUX4* sequence mapping to multiple regions on 4q35.2 and 10q26.3, thus being discarded through the filtering process. The failure of algorithmic analysis to detect *CIC-DUX4* fusions has also been reported by Panagopoulos et al.[27] who applied 3 different programs than ours (FusionMap, FusionFinder, and ChimeraScan). *CIC-DUX4* was not included among their fusion candidates from a SBRCT arising in the thoracic wall of a 40 year-old female, despite the fact that conventional cytogenetics and metaphase FISH showed a t(4;19) (q35;q13). However, using a basic “grep” command searching the fastq sequence data, fusion sequences of *CIC-DUX4* were identified. In fact, no *CIC-DUX4* fusions have been so far identified by fusion discovery programs either from our own RNAseq database or reported in the literature. All documented cases of *CIC-DUX4* fusion positive sarcomas were confirmed mostly by conventional cytogenetics, FISH, and/or RT-PCR methods. In contrast, rare cases of *CIC-FOXO4* fusions in SBRCT and *CIC-LEUTX* fusion in angiosarcoma were detected by RNAseq algorithmic analysis,[24,28,29] suggesting that the 3′ fusion partner, *DUX4*, is the explanation of this pitfall, as discussed above. This hypothesis is further supported by a recently identified group of *DUX4*-rearranged B-cell precursor acute lymphoblastic leukemia, which harbors *IGH-DUX4* or less often *ERG-DUX4* fusions through insertion of part of *DUX4* into the 5′ partner gene.[30] The fusions of *IGH/ERG-DUX4* were detected in only 7 out of 28 positive cases through their standard RNAseq bioinformatics pipeline and required guided analysis to investigate the regions of interest in the remaining cases.

Furthermore, although FISH is commonly used as the diagnostic tool for *CIC*-rearranged tumors, our results highlighted the less than perfect sensitivity of FISH assay, as 6 of our cases with *CIC-DUX4/DUX4-CIC* fusion RNAseq reads by manual inspection were negative for *CIC* rearrangement by FISH. The negative FISH results are most likely related to the subtle, cryptic rearrangements below the FISH resolution. This potential pitfall of cryptic and unbalanced *CIC* rearrangements has been speculated in some unclassified SBRCTs co-expressing WT1 and ETV4 by immunohistochemistry which were negative for *CIC* abnormalities by FISH using the conventional BAC probe design.[4]

In contrast to the inconsistent evidence for a *CIC-DUX4* fusion by either RNAseq or FISH methods, all cases showed high level of *ETV1/4/5* up-regulation. Unsupervised hierarchical clustering also showed that the majority of these samples grouped into a distinct cluster, separate from Ewing sarcoma and *BCOR*-ITD round cell sarcoma, supporting a common transcriptional profile. Our data strongly suggest that the downstream overexpression of *ETV1/4/5* genes has a high sensitivity in the genomic classification of *CIC-DUX4* tumors, compared with FISH and/or RNAseq fusion discovery algorithms. Immunohistochemical staining for ETV4, previously reported to have high sensitivity in other study cohorts,[4,5] was positive in only 64% (7/11) of our cases, which might be related to older or decalcified archival material studied.

An unusual feature of SBRCTs with *CIC-DUX4* fusions is the consistent exonic DNA breakpoint for *CIC*, compared with the prevalent intronic DNA break seen in most other translocation-associated sarcomas. Likewise, all *CIC-FOXO4* and *CIC-LEUTX* fusions reported to date have exonic DNA breakpoints.[24,28,29] Another intriguing finding is that in 2 of our cases, the *CIC-DUX4* fusion resulted in a stop codon right after the fusion junction (case #6, #7). Thus the putative chimeric amino acid sequence consists only of a prematurely truncated CIC protein without a subsequent DUX4 protein. A similar truncation of predicted fusion protein was previously described in 10 *CIC-DUX4* sarcoma cases.[1,3,31,32] Gambarotti et al described 2 *CIC-DUX4* fusion variants with immediate stop codons after the fusion junction.[3] Our case #6 had an identical fusion breakpoint to their case #1 reported, while our case #7 was similar to their case #4, except for one nucleotide difference at the fusion junction (Supporting Information Table 2). The latter fusion variant was also previously reported by our group (case #9).[1] Our findings demonstrate that cases with this fusion variant showed similar morphology and downstream effect of *PEA3* family up-regulation akin to other *CIC-DUX4* fusions variants. The functionality of this truncation type *CIC-DUX4* fusion awaits to be investigated. One hypothesis is that truncation of *CIC* is sufficient to induce tumorigenesis. Another possibility is that this truncation fusion variant coexists with other in-frame fusion transcripts of *CIC-DUX4*. The latter may be supported by the fact that the case previously reported by our group indeed had different fusion variants identified by 3′ rapid amplification of cDNA ends (RACE).[1] All the other 9 cases reported with this fusion variant were identified by RT-PCR using the same primers.[3,31,32] Two of the cases showed overlapping *CIC* and *DUX4* sequences after the presumed *CIC* breakpoints, which could also be explained by the presence of multiple fusion variants.[31,32]

CIC encodes a transcriptional repressor that normally inhibits *ETV1/4/5* expressions and regulates receptor tyrosine kinase signaling pathways.[33,34] CIC siRNA knockdown in human melanoma cell line (SKMEL13), carrying *BRAF* V600E mutation, led to elevated mRNA levels of *ETV1/4/5*.[33] High *ETV1/4/5* expression is also seen in oligodendroglioma with concurrent 1p19q deletion and inactivating mutations of *CIC* (19q13.2), resulting in biallelic disruption of *CIC* gene and loss of CIC protein expression by IHC, presumably due to enhanced degradation of mutant CIC protein.[35,36] In *CIC-DUX4* sarcomas, the *ETV1/4/5* up-regulation may suggest similar *CIC* loss-of-function abnormalities, however, the increased CIC protein expression by western blot is intriguing in the absence of *CIC* mRNA up-regulation and might simply represent accumulation of the truncated or non-functional CIC protein, lacking the repressor domain at its C-terminus.[8,24,34] Similar *ETV1/4/5* up-regulation is also present in other *CIC* related fusions, such as *CIC-LEUTX* positive angiosarcoma and *CIC-NUTM1*-positive central nervous system primitive neuroectodermal tumor (PNET).[24,37] The variable *CIC* gene partners reinforce the hypothesis that the downstream upregulation of *ETV1/4/5* expression is mainly a result of CIC truncation through translocation rather than induced by the encoded sequence of the fused partner.

The exact role in tumorigenesis of *DUX4* dysregulation in the setting of *CIC-DUX4* fusion remains poorly defined. *DUX4* is normally expressed in testis and epigenetically silenced through CpG methylation in differentiated somatic cells.[38] Aberrant expression of DUX4 in primary human myoblasts activates genes associated with stem cell development.[39] Recently, *CIC-DUX4* sarcoma has been shown to have strong DUX4 immunoexpression,

while other round cell sarcomas (i.e., Ewing sarcoma, alveolar/embryonal rhabdomyosarcoma, synovial sarcoma, desmoplastic small round cell tumor) did not.[40] Unfortunately, our data cannot support this finding, since the *DUX4* mRNA expression level cannot be evaluated in our samples due to failure of *DUX4* sequence mapping.

In this study, 7 of 14 SBRCTs showed *CIC-DUX4* fusion junction reads or chimeric reads upon manual inspection of RNAseq data. In 2 additional cases, only the reciprocal *DUX4-CIC* reads but not *CIC-DUX4* were found, suggesting that in some cases, the *CIC-DUX4* transcripts may not be readily amplified through the sequencing process. In fact, in some cases with *CIC-DUX4* reads present, the number of wild-type *CIC* reads outnumbered that of *CIC-DUX4* reads. The fact that *CIC-DUX4* fusion transcripts are not necessarily highly expressed, at least in some cases, might explain why some cases showed *CIC* break-apart by FISH but no evidence of *CIC* alteration by manual inspection of *CIC* reads. The remaining 5 cases lacked *CIC-DUX4/DUX4-CIC* reads, despite the fact that high level of *ETV1/4/5* expression and *CIC* break-apart by FISH were identified. Two of the cases (case #11,12) were also positive for *CIC-DUX4* FISH fusion assay (both fused to 4q35 *DUX4*). There was no significant difference regarding *ETV1/4/5*, *WT1*, and *CIC* mRNA expression levels noted among cases with *CIC-DUX4* reads, *DUX4-CIC* reads, or no fusion reads.

The sensitivity of RT-PCR in diagnosing *CIC-DUX4* tumors remains to be studied and compared with other methodology. In this study, we only validated *CIC-DUX4* and *DUX4-CIC* fusion transcripts by RT-PCR in one case each with available materials. The primers used in each sample were designed based on the known breakpoints from RNAseq manual inspection. Without the known breakpoints, multiple combinations of primers may be needed to cover possible breakpoints reported in *CIC* (scattered in exon 19 and 20) and *DUX4* (exon 1, intron 1, or exon 2), especially when dealing with FFPE tissues. Gambarotti et al. reported 7 *CIC-DUX4* SBRCTs identified by RT-PCR using RNA from frozen tissues.[3] The 7 samples all fell into one of the two fusion variants having different, though close, *CIC* breakpoints and the same *DUX4* breakpoint, in contrast to the more diversely distributed breakpoints found in this study. Although the primers used in their study covered all the breakpoints we found, fusion transcripts with larger amplicons and high GC content may be difficult to amplify, as evidenced by another *CIC-DUX4* SBRCT case report.[27]

Since the entire study cohort showed high *ETV1/4/5* expression, we further evaluated the expression of downstream targets of *ETV1/4/5*.[10–19] Among them only *SPRED2, NOTCH1*, and *CCND2* were up-regulated compared with other soft tissue tumors studied on the same RNAseq platform. *SPRED2* is a negative regulator of Ras/Raf-1/ERK signaling pathway and is also up-regulated in GIST, another tumor with high *ETV1* expression. *NOTCH1* and *CCND2* were reported as downstream targets of *ETV4*.[12,14] NOTCH1 signaling pathway plays an important role in embryonic development, whereas *CCND2* encodes cyclin D2 that controls cell cycle progression from G1 to S phase. Both genes have been implicated in the tumorigenesis of many human cancers.[41–44]

In conclusion, our study demonstrates that a significant number of SBRCT that remain unclassified by whole transcriptome sequencing show a *CIC-DUX4* sarcoma type gene signature, with high levels of *ETV1/4/5*. Our subsequent analysis showed that most of these

cases have *CIC-DUX4* or *DUX4-CIC* reads by RNAseq manual inspection, *CIC* gene rearrangements by FISH, and/or ETV4 immunoexpression in keeping with their classification as *CIC*-fusion positive SBRCTs. Our results further highlight the limitations of the RNAseq algorithm analysis for fusion gene discovery, which consistently fail to detect *CIC-DUX4* fusions, most likely related to the *DUX4* multi-mapping repetitive sequence. Thus, *ETV1/4/5* transcriptional up-regulation shows a very robust sensitivity in diagnosing *CIC-DUX4* sarcomas compared with RNAseq fusion discovery and FISH.

Supplementary Material

Refer to Web version on PubMed Central for supplementary material.

Acknowledgments

Funding information

P50 CA140146-01 (CRA); P30 CA008748 (CRA); Kristen Ann Carr Foundation (CRA); Cycle for Survival (CRA); Kuwait Medical Genetics Centre, Ministry of Health, Kuwait (AA).

References

1. Italiano A, Sung YS, Zhang L, et al. High prevalence of CIC fusion with double-homeobox (DUX4) transcription factors in EWSR1-negative undifferentiated small blue round cell sarcomas. Genes Chromosomes Cancer. 2012; 51:207–218. [PubMed: 22072439]
2. Specht K, Sung YS, Zhang L, et al. Distinct transcriptional signature and immunoprofile of CIC-DUX4 fusion-positive round cell tumors compared with EWSR1-rearranged Ewing sarcomas: further evidence toward distinct pathologic entities. Genes Chromosomes Cancer. 2014; 53:622–633. [PubMed: 24723486]
3. Gambarotti M, Benini S, Gamberi G, et al. CIC-DUX4 fusion-positive round-cell sarcomas of soft tissue and bone: a single-institution morphological and molecular analysis of seven cases. Histopathology. 2016; 69:624–634. [PubMed: 27079694]
4. Hung YP, Fletcher CD, Hornick JL. Evaluation of ETV4 and WT1 expression in CIC-rearranged sarcomas and histologic mimics. Mod Pathol. 2016; 29:1324–1334. [PubMed: 27443513]
5. Le Guellec S, Velasco V, Perot G, Watson S, Tirode F, Coindre JM. ETV4 is a useful marker for the diagnosis of CIC-rearranged undifferentiated round-cell sarcomas: a study of 127 cases including mimicking lesions. Mod Pathol. 2016; 29:1523–1531. [PubMed: 27562494]
6. Yoshida A, Goto K, Kodaira M, et al. CIC-rearranged sarcomas: a study of 20 cases and comparisons with ewing sarcomas. Am J Surg Pathol. 2016; 40:313–323. [PubMed: 26685084]
7. Choi EY, Thomas DG, McHugh JB, et al. Undifferentiated small round cell sarcoma with t(4;19)(q35;q13.1) CIC-DUX4 fusion: a novel highly aggressive soft tissue tumor with distinctive histopathology. Am J Surg Pathol. 2013; 37:1379–1386. [PubMed: 23887164]
8. Kawamura-Saito M, Yamazaki Y, Kaneko K, et al. Fusion between CIC and DUX4 up-regulates PEA3 family genes in Ewing-like sarcomas with t(4;19)(q35;q13) translocation. Hum Mol Genet. 2006; 15:2125–2137. [PubMed: 16717057]
9. Smith SC, Palanisamy N, Martin E, et al. The utility of etv1, etv4, and etv5 rna in situ hybridization in the diagnosis of cic-dux4 sarcomas. Histopathology. 2017; 70:657–663. [PubMed: 27790742]
10. Chi P, Chen Y, Zhang L, et al. ETV1 is a lineage survival factor that cooperates with KIT in gastrointestinal stromal tumours. Nature. 2010; 467:849–853. [PubMed: 20927104]
11. Keld R, Guo B, Downey P, Gulmann C, Ang YS, Sharrocks AD. The ERK MAP kinase-PEA3/ETV4-MMP-1 axis is operative in oesophageal adenocarcinoma. Mol Cancer. 2010; 9:313. [PubMed: 21143918]

12. Clementz AG, Rogowski A, Pandya K, Miele L, Osipo C. NOTCH-1 and NOTCH-4 are novel gene targets of PEA3 in breast cancer: novel therapeutic implications. Breast Cancer Res. 2011; 13:R63. [PubMed: 21679465]
13. Oh S, Shin S, Janknecht R. ETV1, 4 and 5: an oncogenic subfamily of ETS transcription factors. Biochim Biophys Acta. 2012; 1826:1–12. [PubMed: 22425584]
14. Ladam F, Damour I, Dumont P, et al. Loss of a negative feedback loop involving pea3 and cyclin d2 is required for pea3-induced migration in transformed mammary epithelial cells. Mol Cancer Res. 2013; 11:1412–1424. [PubMed: 23989931]
15. Li S, Huang X, Zhang D, et al. Requirement of PEA3 for transcriptional activation of FAK gene in tumor metastasis. PLoS One. 2013; 8:e79336. [PubMed: 24260201]
16. Verger A, Baert JL, Verreman K, et al. The Mediator complex subunit MED25 is targeted by the N-terminal transactivation domain of the PEA3 group members. Nucleic Acids Res. 2013; 41:4847–4859. [PubMed: 23531547]
17. Park SW, Do HJ, Ha WT, et al. Transcriptional activation of OCT4 by the ETS transcription factor PEA3 in NCCIT human embryonic carcinoma cells. FEBS Lett. 2014; 588:3129–3136. [PubMed: 24983502]
18. Harada H, Omi M, Sato T, Nakamura H. Pea3 determines the isthmus region at the downstream of Fgf8-Ras-ERK signaling pathway. Dev Growth Differ. 2015; 57:657–666. [PubMed: 26691276]
19. Kherrouche Z, Monte D, Werkmeister E, et al. PEA3 transcription factors are downstream effectors of Met signaling involved in migration and invasiveness of Met-addicted tumor cells. Mol Oncol. 2015; 9:1852–1867. [PubMed: 26238631]
20. Feng Q, Snider L, Jagannathan S, et al. A feedback loop between nonsense-mediated decay and the retrogene DUX4 in facioscapulohumeral muscular dystrophy. Elife. 2015; 4:e4996.
21. Lim JW, Snider L, Yao Z, et al. DICER/AGO-dependent epigenetic silencing of D4Z4 repeats enhanced by exogenous siRNA suggests mechanisms and therapies for FSHD. Hum Mol Genet. 2015; 24:4817–4828. [PubMed: 26041815]
22. Bao B, Maruyama R, Yokota T. Targeting mRNA for the treatment of facioscapulohumeral muscular dystrophy. Intractable Rare Dis Res. 2016; 5:168–176. [PubMed: 27672539]
23. Jones TI, Parilla M, Jones PL. Transgenic drosophila for investigating DUX4 and FRG1, two genes associated with facioscapulohumeral muscular dystrophy (FSHD). PLoS One. 2016; 11:e0150938. [PubMed: 26942723]
24. Huang SC, Zhang L, Sung YS, et al. Recurrent CIC gene abnormalities in angiosarcomas: a molecular study of 120 cases with concurrent investigation of plcg1, kdr, myc, and flt4 gene alterations. Am J Surg Pathol. 2016; 40:645–655. [PubMed: 26735859]
25. van der Maarel SM, Frants RR. The D4Z4 repeat-mediated pathogenesis of facioscapulohumeral muscular dystrophy. Am J Hum Genet. 2005; 76:375–386. [PubMed: 15674778]
26. Sboner A, Habegger L, Pflueger D, et al. FusionSeq: a modular framework for finding gene fusions by analyzing paired-end RNA-sequencing data. Genome Biol. 2010; 11:R104. [PubMed: 20964841]
27. Panagopoulos I, Gorunova L, Bjerkehagen B, Heim S. The “grep” command but not FusionMap, FusionFinder or ChimeraScan captures the CIC-DUX4 fusion gene from whole transcriptome sequencing data on a small round cell tumor with t(4;19)(q35;q13). PLoS One. 2014; 9:e99439. [PubMed: 24950227]
28. Brohl AS, Solomon DA, Chang W, et al. The genomic landscape of the Ewing Sarcoma family of tumors reveals recurrent STAG2 mutation. PLoS Genet. 2014; 10:e1004475. [PubMed: 25010205]
29. Sugita S, Arai Y, Tonooka A, et al. A novel CIC-FOXO4 gene fusion in undifferentiated small round cell sarcoma: a genetically distinct variant of Ewing-like sarcoma. Am J Surg Pathol. 2014; 38:1571–1576. [PubMed: 25007147]
30. Lilljebjorn H, Henningsson R, Hyrenius-Wittsten A, et al. Identification of ETV6-RUNX1-like and DUX4-rearranged subtypes in paediatric B-cell precursor acute lymphoblastic leukaemia. Nat Commun. 2016; 7:11790. [PubMed: 27265895]
31. Machado I, Cruz J, Lavernia J, et al. Superficial EWSR1-negative undifferentiated small round cell sarcoma with CIC/DUX4 gene fusion: a new variant of Ewing-like tumors with locoregional lymph node metastasis. Virchows Arch. 2013; 463:837–842. [PubMed: 24213312]

32. Bielle F, Zanello M, Guillemot D, et al. Unusual primary cerebral localization of a CIC-DUX4 translocation tumor of the Ewing sarcoma family. Acta Neuropathol. 2014; 128:309–311. [PubMed: 24980961]
33. Dissanayake K, Toth R, Blakey J, et al. ERK/p90(RSK)/14-3-3 signalling has an impact on expression of PEA3 Ets transcription factors via the transcriptional repressor capicua. Biochem J. 2011; 433:515–525. [PubMed: 21087211]
34. Jimenez G, Shvartsman SY, Paroush Z. The Capicua repressor-a general sensor of RTK signaling in development and disease. J Cell Sci. 2012; 125:1383–1391. [PubMed: 22526417]
35. Gleize V, Alentorn A, Connen de Kerillis L, et al. CIC inactivating mutations identify aggressive subset of 1p19q codeleted gliomas. Ann Neurol. 2015; 78:355–374. [PubMed: 26017892]
36. Padul V, Epari S, Moiyadi A, Shetty P, Shirsat NV. ETV/Pea3 family transcription factor-encoding genes are overexpressed in CIC-mutant oligodendrogliomas. Genes Chromosomes Cancer. 2015; 54:725–733. [PubMed: 26357005]
37. Sturm D, Orr BA, Toprak UH, et al. New brain tumor entities emerge from molecular classification of CNS-PNETs. Cell. 2016; 164:1060–1072. [PubMed: 26919435]
38. Krom YD, Thijssen PE, Young JM, et al. Intrinsic epigenetic regulation of the D4Z4 macrosatellite repeat in a transgenic mouse model for FSHD. PLoS Genet. 2013; 9:e1003415. [PubMed: 23593020]
39. Geng LN, Yao Z, Snider L, et al. DUX4 activates germline genes, retroelements, and immune mediators: implications for facioscapulohumeral dystrophy. Dev Cell. 2012; 22:38–51. [PubMed: 22209328]
40. Siegele B, Roberts J, Black JO, Rudzinski E, Vargas SO, Galambos C. DUX4 Immunohistochemistry is a Highly Sensitive and Specific Marker for CIC-DUX4 Fusion-positive Round Cell Tumor. Am J Surg Pathol. 2017; 41:423–429. [PubMed: 27879517]
41. Rota R, Ciarapica R, Miele L, Locatelli F. Notch signaling in pediatric soft tissue sarcomas. BMC Med. 2012; 10:141. [PubMed: 23158439]
42. Capaccione KM, Pine SR. The Notch signaling pathway as a mediator of tumor survival. Carcinogenesis. 2013; 34:1420–1430. [PubMed: 23585460]
43. Kawano M, Tanaka K, Itonaga I, Iwasaki T, Tsumura H. c-Myc represses tumor-suppressive micrornas, let-7a, mir-16 and mir-29b, and induces cyclin d2-mediated cell proliferation in ewing's sarcoma cell line. PLoS One. 2015; 10:e0138560. [PubMed: 26393798]
44. Misiewicz-Krzeminska I, Sarasquete ME, Vicente-Duenas C, et al. Post-transcriptional modifications contribute to the upregulation of cyclin d2 in multiple myeloma. Clin Cancer Res. 2016; 22:207–217. [PubMed: 26341922]

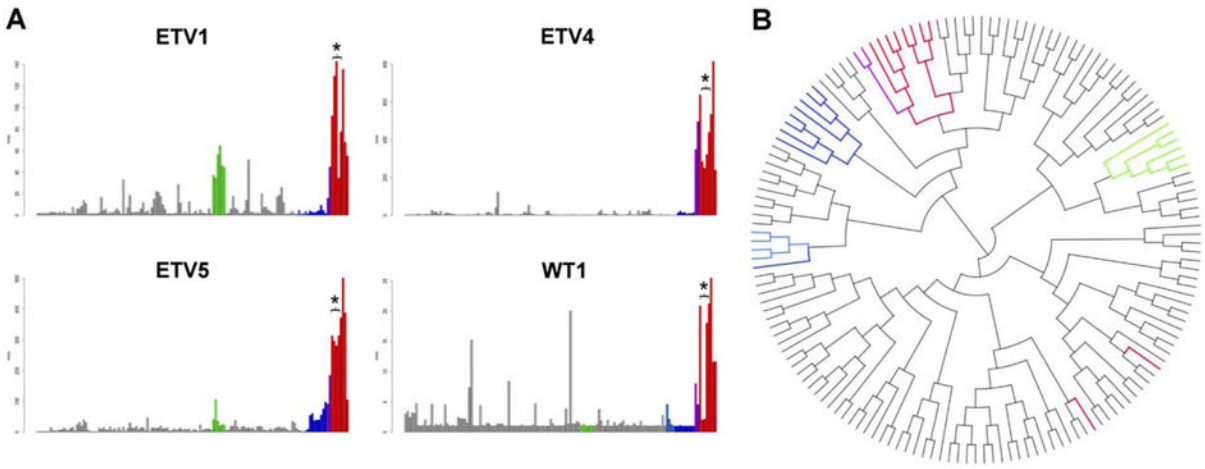

FIGURE 1.

(A) High level of *ETV1*, *ETV4*, *ETV5*, and *WT1* mRNA overexpression identified in the study cohort (red), compared with the non-*CIC* SBRCT group (Ewing sarcoma, SBRCT with *BCOR* ITD, *YWHAE-NUTM2B*, or *BCOR-CCNB3*; dark blue), Ewing sarcoma cell lines (light blue), GIST (green) and other soft tissue tumors (gray) studied on the same RNAseq platform. Similarly, 2 angiosarcomas with *CIC* rearrangements (purple) showed moderate increased expression, especially for *ETV4*. GIST had upregulation restricted to *ETV1*. Asterisks indicate the 4 cases negative for ETV4 immunostaining, which showed upregulated mRNA expressions of *ETV4*, as well as *ETV1* and *ETV5*, compared with other tumor types. **(B)** By unsupervised hierarchical clustering, the study cohort (red) and the 2 angiosarcomas with *CIC* rearrangements (purple) grouped together in keeping with a closely related transcriptional profile, separate from other SBRCTs with *BCOR* ITD, *YWHAE-NUTM2B*, or *BCOR-CCNB3*, Ewing sarcomas (dark blue), Ewing sarcomas cell lines (light blue), and GIST (green). [Color figure can be viewed at wileyonlinelibrary.com]

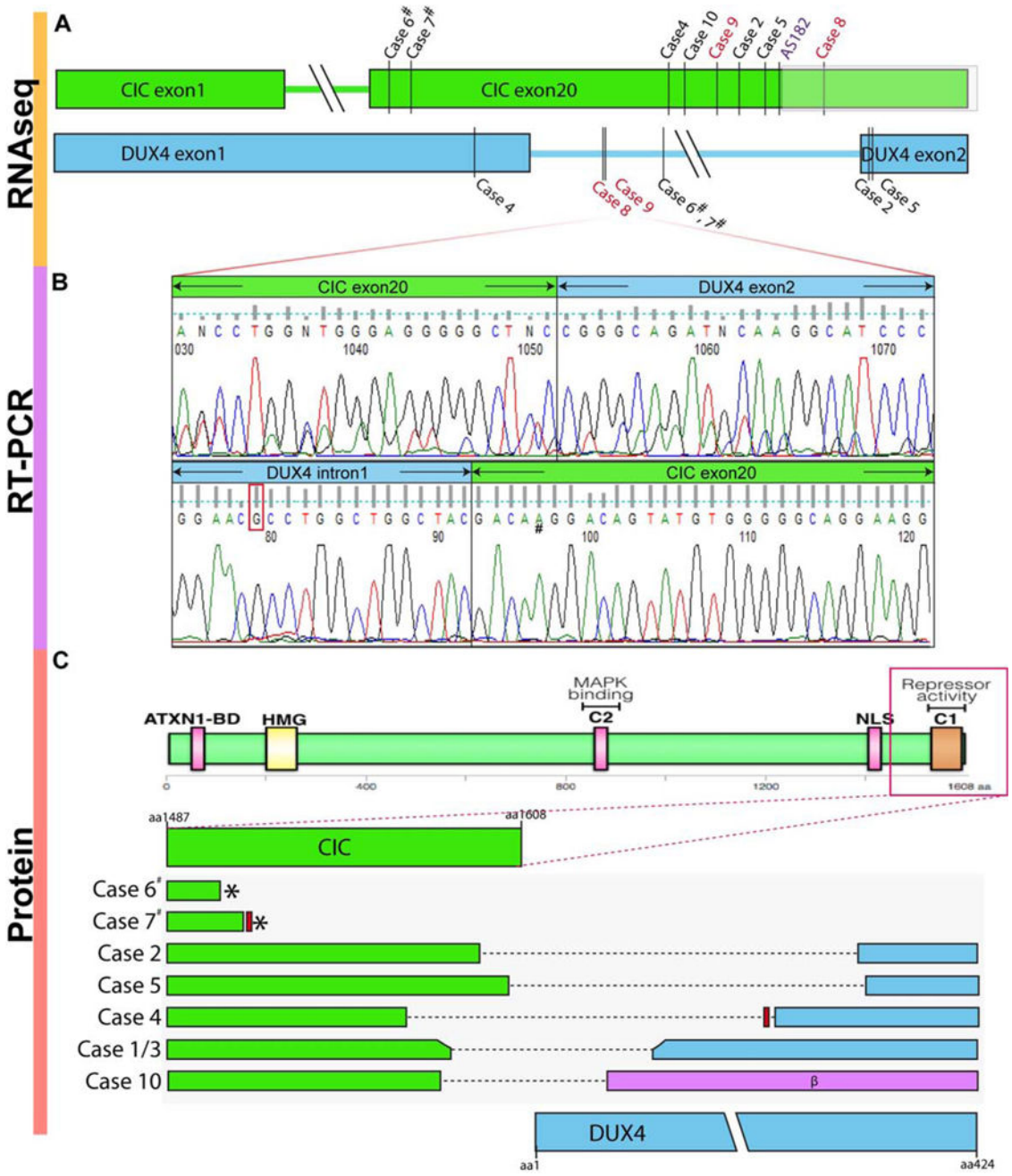

FIGURE 2.

Schematic breakpoint diagrams in various *CIC-DUX4* and *DUX4-CIC* fusion transcripts (A,B), and projected chimeric proteins related to the protein domains of CIC (C). **(A)** The *CIC* breakpoint was located in the last *CIC* exon (exon 20) in all cases evaluable, either from the *CIC-DUX4* reads (black) and *DUX4-CIC* reads (red) identified by RNAseq manual inspection or by the RNAseq algorithm in the angiosarcoma with *CIC-LEUTX* fusion (purple). (#, cases with stop codon after the fusion junction, as previously reported[1,3,31]). The *DUX4* breakpoints were distributed in exon 1, intron 1, and exon 2. Cases #1 & 3 (not shown) had only chimeric reads, thus the exact breakpoints could not be established. **(B)**

CIC-DUX4 and *DUX4-CIC* fusion transcripts confirmed by RT-PCR in cases #2 and #8, respectively. Case #8 showed a *DUX4* break within intron 1, which was fused to *CIC* exon 20 (3′ UTR region), with an additional T to A nucleotide change in *CIC* (#). The *DUX4* sequence contains the nucleotide G (marked), confirming its origin from chromosome 10. As both breakpoints occurred in non-coding region, there is no predicted amino acid sequence. **(C)** Wild-type CIC protein domains, including ATXN1 binding domain (ATXN1-BD), high mobility group (HMG) box for DNA binding, C2 for MAPK binding, nuclear localization signal (NLS) domain, and C1 domain with repressor activity, are shown on the top.[33,34] *CIC* exon 20 encodes the C1 domain with repressor activity. Truncated CIC proteins lacking encoding DUX4 sequence were predicted for cases #6 and 7 with a stop codon (*) right after the fusion junction. The narrow red bar following the truncated CIC in case #7 indicates an amino acid (Alanine) derived from the fusion junction before the stop codon. Wedge-shaped bars represent cases with only *CIC-DUX4* chimeric reads available; thus the projected protein length is approximated. Case #4 had an extra amino acid (Glycine) (red bar) due to 3 nucleotides (GGG) insertion at the fusion junction. Case #10 showed *CIC* fused to an un-annotated region on chromosome 17 (genomic position: 41419677) (purple bar labeled with b). [Color figure can be viewed at wileyonlinelibrary.com]

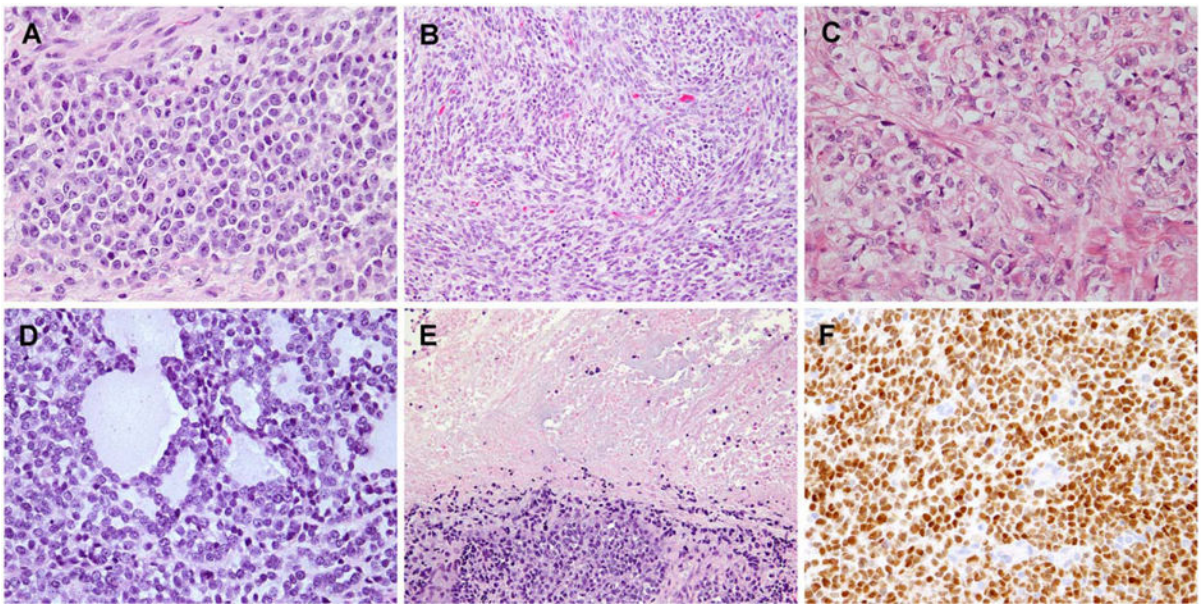

FIGURE 3.

Histologic findings of SBRCTs with PEA3 gene signature. **(A)** Most cases were composed of sheets of small blue round cells with vesicular chromatin, prominent nucleoli, and mild variation in nuclear size and shape. Uncommon findings included a spindle cell component **(B)** and epithelioid cells with abundant cytoplasm **(C)**. Small to moderate amount of myxoid material was frequently observed, either among tumor cells or forming microcystic spaces **(D)**, or admixed with necrotic debris **(E)**. Immunohistochemical stains for ETV4 were positive in 7 of 11 cases **(F)**. [Color figure can be viewed at wileyonlinelibrary.com]

TABLE 1

Comparison between different approaches to identify *CIC-DUX4* fusions

Case	Age/Sex Location	RNAseq-manual inspection (coding frame)	RNAseq-algorithm analysis	*CIC* FISH	ETV4 IHC	RNAseq-*ETV1/4/5* upregulation
1[a]	29F Thigh	*CIC-DUX4* (chimeric)	N	N	NA	Pos
2[a]	25F Thigh	*CIC-DUX4* (in-frame)	N	N	Pos	Pos
3[a]	58F Paraspinal	*CIC-DUX4* (chimeric)	N	Pos	NA	Pos
4[a]	16F Back	*CIC-DUX4* (in-frame)	N	N	N	Pos
5[a]	12M Proximal phalanx big toe	*CIC-DUX4* (in-frame)	N	NA(decal)	N	Pos
6[b]	17M Buttock	*CIC-DUX4* (STOP codon)	N	Pos	Pos	Pos
7[b]	15F Brain	*CIC-DUX4* (STOP codon)	N	N	Pos	Pos
8[a]	66M Neck	*DUX4-CIC*	N	N	NA	Pos
9[a]	17F Forehead	*DUX4-CIC*	N	N	N	Pos
10[a,b]	21M Neck	N[c]	N	Pos	Pos	Pos
11[a]	66F Arm	N	N	Pos[d]	N	Pos
12[a]	59M Back	N	N	Pos[d]	Pos	Pos
13[b]	15M Back	N	N	Pos	Pos	Pos
14[b]	43M Thigh	N	N	Pos	Pos	Pos

[a]Whole transcriptome sequencing.

[b]Targeted RNA sequencing.

[c]With *CIC* fusion to un-annotated region in chromosome 17.

[d]Fusion FISH assay showed *CIC* fused to *DUX4* (4q35).

IHC, immunohistochemistry; F, female; M, male; N, negative; Pos, positive; NA, not available; decal, tissue decalcification.